

# Steady-State Performance Characteristics of a DC Motor fed by Quadratic DC-DC Boost Converter

M. Vanitha<sup>1</sup>, Dr. D. Murali<sup>2</sup>

<sup>1</sup>PG Scholar, Department of EEE, Government College of Engineering, Salem, Tamil Nadu, India, vanitha028eee@gmail.com

<sup>2</sup>Professor, Department of EEE, Government College of Engineering, Salem, Tamil Nadu, India, muraliems@gmail.com

Received Date : May 8 , 2022    Accepted Date : May 31, 2022    Published Date : June 07, 2022

## ABSTRACT

This paper presents the analysis of steady-state performance of a DC motor fed by a non-isolated quadratic DC-DC boost converter. The proposed quadratic configuration based non-isolated high voltage gain DC-DC converter operating in continuous conduction mode employs one power switch and reduced number of diodes and passive components. Due to single power switch, the switching and conduction losses are reduced thereby improving the converter efficiency. A DC shunt motor of 5 HP power rating is used as load to the proposed converter. The proposed cost-effective converter-fed DC motor operating under no-load is simulated using MATLAB / SIMULINK tool. The steady-state performance characteristics, such as speed, torque, and armature current of the DC motor, are obtained for one particular value of duty ratio of the power switch. The results validate the superior performance of the suggested DC-DC converter-fed DC motor at moderate duty ratio.

**Key words:** Continuous conduction mode, Duty ratio, MATLAB/SIMULINK, Quadratic DC-DC boost converter, Steady-state Performance characteristics, Voltage gain.

## 1. INTRODUCTION

In the last two decades, the researchers focus on the development of new high-gain DC-DC power electronic converters due to the growth of renewable energy. There are many number of improved DC-DC boost converter topologies belonging to isolated and non-isolated structures shown in the literature [1]-[7]. The transformer-based (isolated) topologies have certain drawbacks such as the production of voltage spikes due to the presence of leakage inductance of the transformer, electromagnetic interference (EMI) issues, and complicated control strategy and structure. However, the highly efficient and high-gain non-isolated configurations do not involve the use of transformers and have simplified

structure and control, which make it more desirable for certain applications such as electric vehicles (EVs) [8]-[9]. Some authors recently developed certain non-isolated DC-DC converter topologies with high voltage gain capability [10]-[12]. The hybrid single-switch quadratic boost-Cuk converter structure proposed in [10] can achieve very high voltage gain. But, it suffers from the drawback that the number of passive components used in the structure is large thereby increasing the cost. The converter structure proposed in [11] can achieve very high voltage gain at moderate duty ratio of the power switch. However, it too has a drawback of larger passive component count than that of the structure presented in [10]. The basic interleaved converter topology integrated with multiplier cells presented in [12] has the capability to achieve very high voltage gain. However, the configuration presented in [12] has two power switches and large number of diodes and passive components. Hence, a high voltage gain DC-DC boost converter with reduced component count is developed based on the concept of quadratically increasing output voltage with increasing duty ratio [13].

In this paper, a non-isolated single-switch quadratic DC-DC boost converter with reduced number of diodes and passive components, that feeds a DC shunt motor load, is presented. The proposed converter in this research work has the capability to achieve high steady state DC voltage gain at low value of duty ratio (D). Moreover, the suggested converter operates under continuous inductor current mode. The use of single power switch reduces both the switching and conduction losses and hence the converter efficiency is improved. All the active and passive components used in the power circuit of the converter are assumed to be ideal. A DC shunt motor of 5 HP power rating is energized by the output voltage of the proposed DC-DC converter. MATLAB / SIMULINK tool is used as the platform for simulating the proposed DC-DC converter-fed DC motor. The steady state performance characteristics such as speed, torque, and armature current of the DC motor operating under no-load are validated at low value of duty ratio (D).

The remaining sections of the paper are arranged as follows: Section 2 explains the principle of operation of the proposed DC-DC boost converter and the conventional speed control schemes for the DC shunt motor. Section 3 describes the MATLAB/SIMULINK model of the converter-fed DC motor and the relevant no-load steady-state waveforms of the motor. The concluding section 4 elaborates on the importance of the work.

## 2. PROPOSED DC-DC CONVERTER-FED DC MOTOR

The power circuit of the proposed quadratic high-gain DC-DC boost converter supplying a DC shunt motor load is shown in Fig. 1. The proposed single-switch converter is operating in continuous inductor current mode. The high DC output voltage is obtained from the converter at low duty ratio (D) itself. The ideal active and passive components are used in the power circuit. The modes of operation of the converter [13] and the speed control schemes of the DC shunt motor [14] are explained briefly in the following sections:

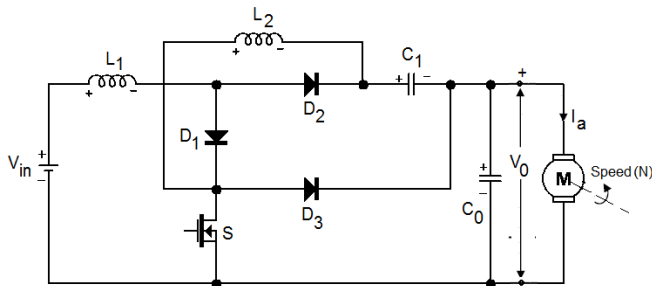


**Figure 1:** Power circuit of the proposed quadratic DC-DC boost converter

### 2.1 Working of the proposed quadratic DC-DC converter

During mode-I operation of the converter, the power switch (MOSFET) is turned ON by a gate pulse. The diode  $D_1$  is forward biased and the diodes  $D_2$  and  $D_3$  get reverse biased. Hence, the diode  $D_1$  acts as short circuit and the diodes  $D_2$  and  $D_3$  act as open circuit. The inductor  $L_1$  is magnetized due to the current flow  $I_{L1}$  through it. The inductor  $L_1$  gets charged to the input voltage  $V_{in}$ . The inductor  $L_2$  is also magnetized by the current  $I_{L2}$  due to the discharge of capacitor  $C_1$ . The voltage across the inductor  $L_2$  is same as the capacitor voltage  $V_{C1}$ . The capacitor  $C_0$  supplies the load current  $I_a$  and hence an output voltage  $V_0$  is obtained across the motor. The current through the power switch  $S$  is the algebraic sum of the currents  $I_{L1}$  and  $I_{L2}$ . The voltages across the inductors  $L_1$  and  $L_2$  are given by Eq.(1).

$$\left. \begin{aligned} V_{L1,ON} &= V_{in} \\ V_{L2,ON} &= V_{C1} \end{aligned} \right\} \quad (1)$$

During mode-II operation of the converter, the switch  $S$  is turned OFF. The diode  $D_1$  is reverse biased. So the diode  $D_1$  gets open circuited. The diodes  $D_2$  and  $D_3$  get forward biased. So the diodes  $D_2$  and  $D_3$  get short circuited. The inductors  $L_1$  and  $L_2$  release the stored energy and hence charge the capacitors  $C_1$  and  $C_0$ . During mode-II, the voltages across the

inductors  $L_1$  and  $L_2$  are represented by Eq.(2).

$$\left. \begin{aligned} V_{L1,OFF} &= V_{in} - V_{C1} \\ V_{L2,OFF} &= V_{C1} - V_0 \end{aligned} \right\} \quad (2)$$

The fundamental volt-second balance concept is applied for the two inductors and finally the voltage gain (G) equation is derived for the proposed quadratic DC-DC boost converter with duty ratio  $D$  for the power switch  $S$  as shown below [13]:

$$G = \frac{V_0}{V_{in}} = \frac{1}{(1-D)^2} \quad (3)$$

### 2.2 Methods of speed control of DC shunt motor

DC motors are most suitable for wide range speed control and are therefore indispensable for many adjustable speed drives [14]. The speed ( $\omega_m$ ) of a DC motor is given by Eq.(4).

$$\omega_m = \frac{V - I_a r_a}{K_a \phi} \quad (4)$$

where armature constant  $K_a = \frac{PZ}{2\pi a}$  and  $\phi$  is the field flux

per pole,  $V$  is the applied armature voltage,  $I_a$  is the armature current,  $r_a$  is the armature winding resistance,  $P$  is the number of field poles,  $Z$  is the number of armature winding conductors,  $a$  is the number of parallel paths in the armature winding.

It follows from Eq.(4) that for a DC motor, there are basically three methods of speed control and these are:

(i). Variation of resistance in the armature circuit:

In this method, an external resistance is inserted in series with the armature circuit to obtain speeds below the base speed only. The disadvantages of this method are: lower efficiency and higher operational costs at reduced speeds; poor speed regulation with fixed controller resistance in the armature circuit.

ii). Variation of the field flux,

This method of speed control gives the speeds above the base speed only. The field flux and hence the speed of a DC shunt motor can be controlled easily by varying the field regulating resistance. This is one of the simplest and economical methods. The disadvantages of this method are: top speeds are obtained with very weak field; the armature may get overheated at high speeds; if the field flux is weakened considerably, the speed becomes very high.

(iii). Variation of the armature terminal voltage:

In this method, if the armature terminal voltage  $V$  is varied, the counter emf ( $V - I_a r_a$ ) changes almost proportionally and for a constant-flux motor (for example, a DC shunt motor), the speed changes approximately in the same proportion as  $V$ .

In the proposed research work, the armature terminal voltage control method is used for the speed control of the DC motor fed by the proposed quadratic DC-DC boost converter. The

no-load operation of the motor with constant field current is considered. The armature voltage ( $V_0$ ) of the motor is obtained by varying the input voltage ( $V_{in}$ ) for a fixed value of duty ratio (D). Thus, the speed of the given motor can be controlled. The duty ratio (D) of the power switch S can be varied in order to obtain the variable speed operation of the motor for the different values of armature voltage ( $V_0$ ).

**3. SIMULATION OF THE PROPOSED CONVERTER-FED DC MOTOR AND THE RESULTS**

The MATLAB / SIMULINK model of the proposed quadratic DC-DC boost converter-fed DC shunt motor is shown in Fig. 2. The no-load operation of the DC shunt motor is considered in the study. The circuit components are obtained from the Sim Power System library. The simulation model parameters

and the specifications of the proposed quadratic DC-DC boost converter-fed DC shunt motor are shown in Table 1. Table 2 shows the speed variations of the motor with respect to changes in duty ratio (D) and hence the armature voltage. The sampling period  $T_s = 4e^{-005}$  s, graphical user interface (GUI), and ‘ode 45’ solver are used for simulating the converter-fed DC motor model. A gate pulse as shown in Fig. 3 is used for triggering the MOSFET switch S into conduction. The waveforms of the converter input voltage ( $V_{in}$ ), converter input current ( $I_{in}$ ), output voltage ( $V_0$ ), output current ( $I_0$ ), armature current ( $I_a$ ), field current ( $I_f$ ), speed ( $\omega_m$ ), electromagnetic torque ( $T_e$ ), duty ratio versus armature voltage, and armature voltage versus speed are shown in Fig. 4, Fig. 5, Fig. 6, Fig. 7, Fig. 8, Fig. 9, Fig. 10, Fig. 11, Fig. 12, and Fig. 13 respectively for the duty factor D = 0.71.

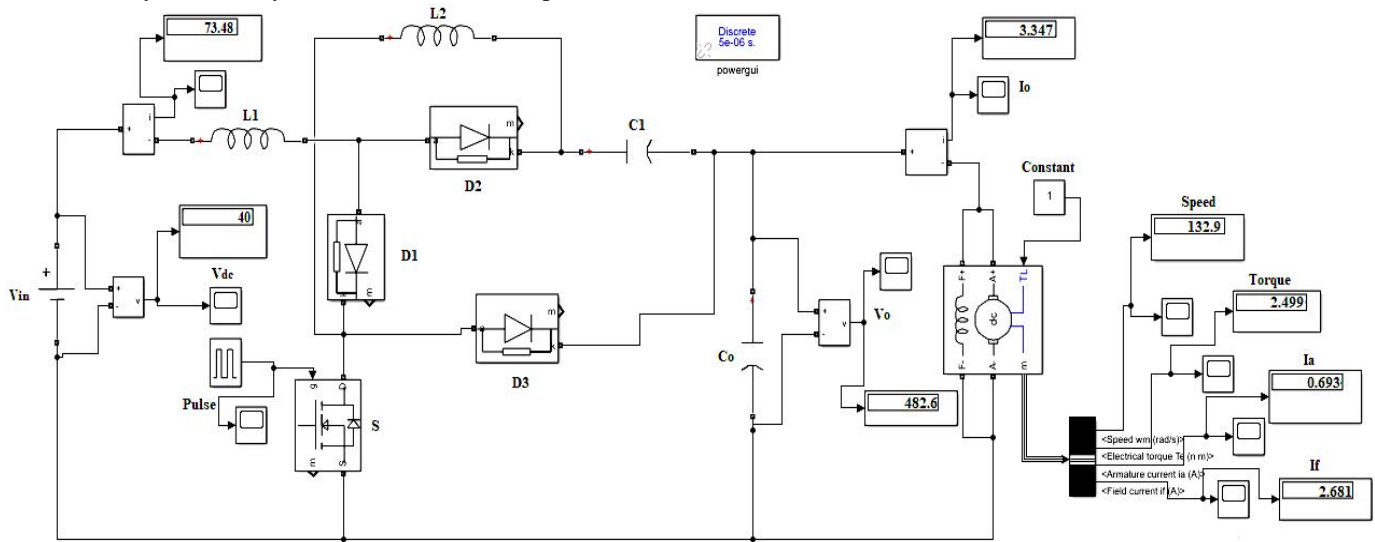


Figure 2: Simulation model of the proposed quadratic DC-DC converter-fed DC motor

Table 1: Simulation parameters of the proposed quadratic boost DC-DC converter

Parameters/Specifications	Values
Inductor ( $L_1, L_2$ )	400 mH, 100 mH
Capacitors ( $C_1, C_0$ )	100 $\mu$ F, 5000 $\mu$ F
Armature winding resistance ( $r_a$ )	1 $\Omega$
Duty factor (D) of the power MOSFET switch ‘S’	0.71
Switching frequency ( $f_s$ )	50 kHz
Converter input voltage ( $V_{in}$ )	40 V
Converter output voltage ( $V_0$ )	483 V
Power rating of the DC shunt motor	10 HP
Armature winding specifications	500 V, 17 A
Field winding specifications	240 V, 1.7 A
Speed of the motor	1750 rpm

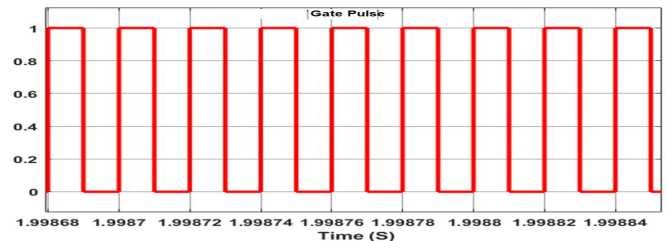
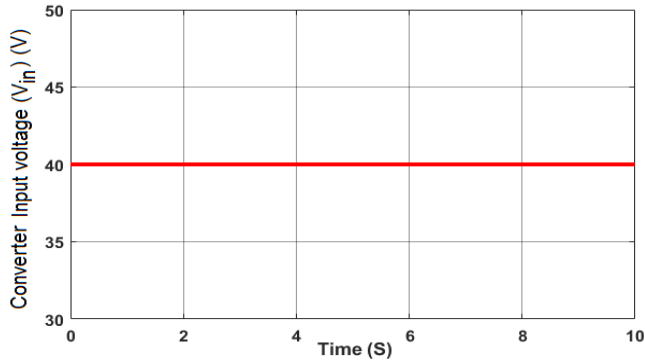


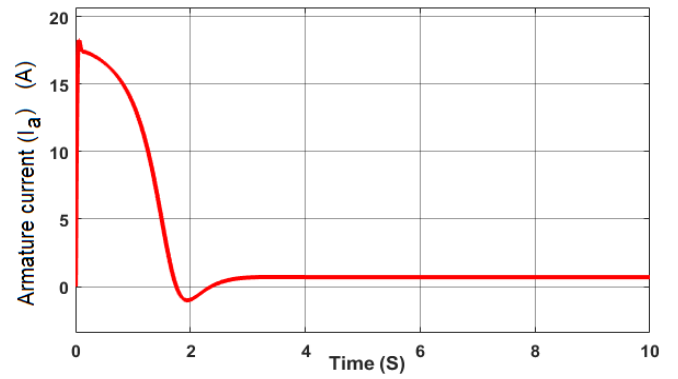
Figure 3: Gate pulse to the power MOSFET (S)

Table 2: Speed variations of the motor with respect to duty ratio (D)

Duty ratio (D)	Armature voltage ( $V_a$ ) (V)	Speed (rpm)
0.40	128	1159
0.45	141	1178
0.50	153	1193
0.55	202	1242
0.59	235	1248
0.63	293	1254
0.66	348	1261
0.71	482	1269
0.75	498	1269



**Figure 4:** Converter input voltage ( $V_{in}$ )



**Figure 8:** Armature current ( $I_a$ )

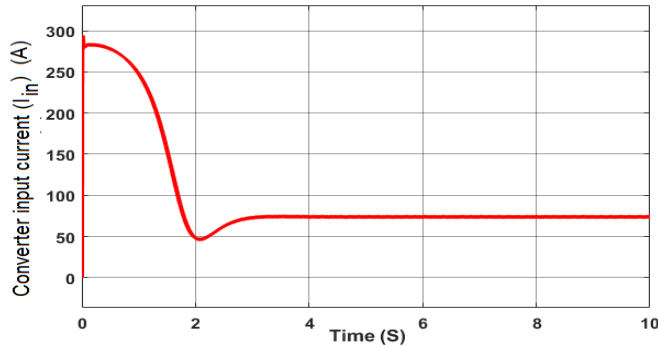


**Figure 5:** Converter input current ( $I_{in}$ )

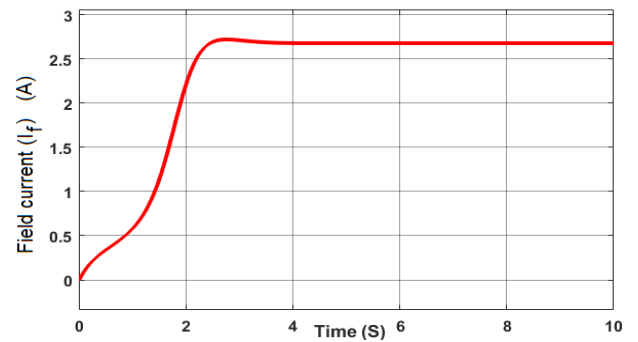


**Figure 9:** Field current ( $I_f$ )

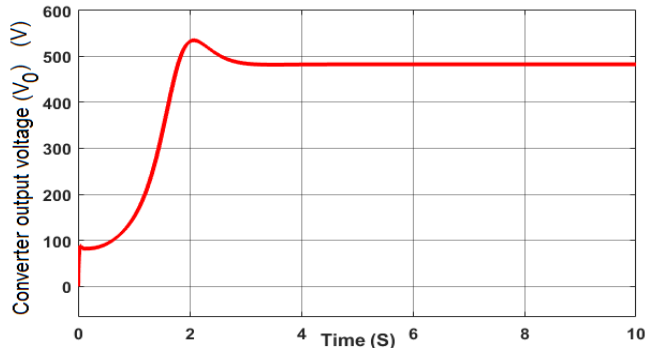


**Figure 6:** Converter output voltage ( $V_o$ )

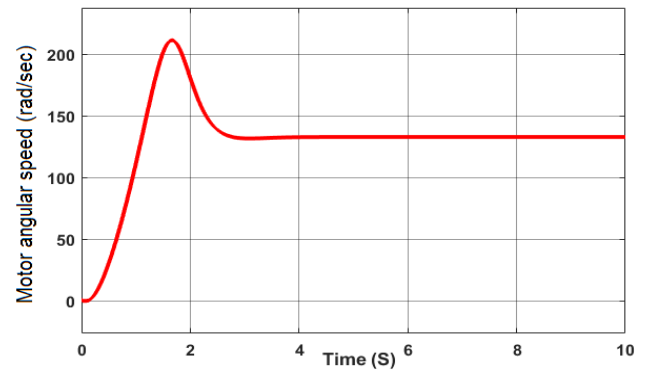


**Figure 10:** Motor angular speed ( $\omega_m$ )

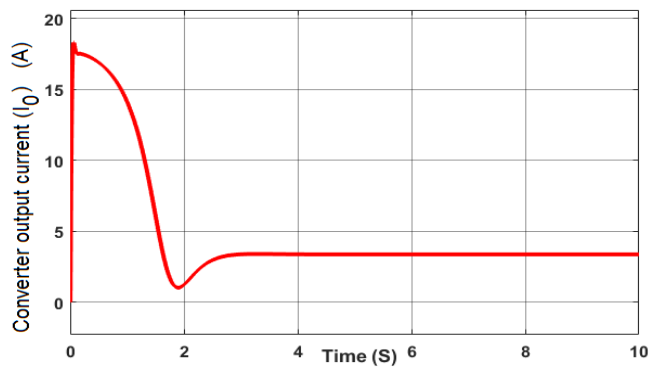


**Figure 7:** Converter output current ( $I_o$ )

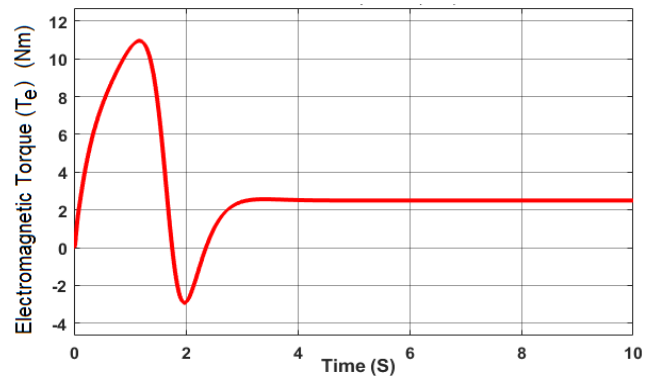


**Figure 11:** Electromagnetic torque ( $T_e$ ) of the motor

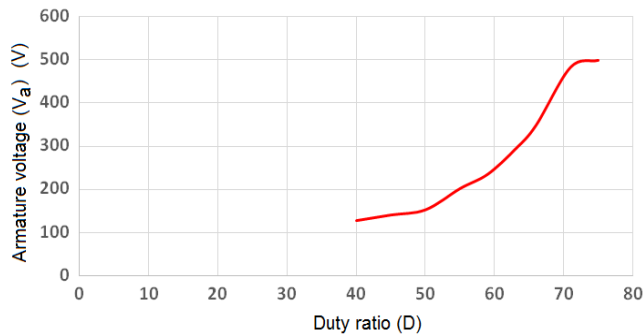


Figure 12: Variation of armature voltage with Duty ratio

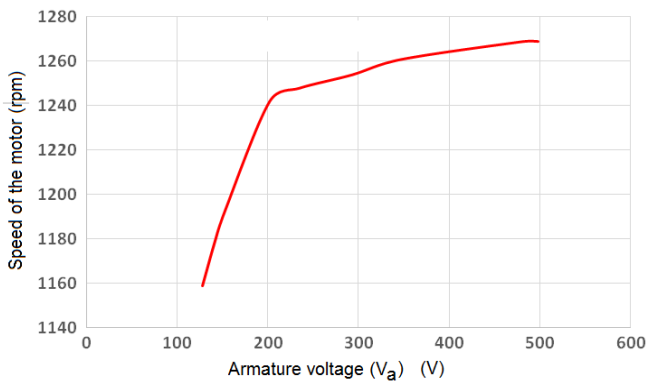


Figure 13: Variation of motor speed with armature voltage

#### 4. CONCLUSION

In this research article, the steady-state performance characteristics of a DC shunt motor fed by a non-isolated high-gain quadratic single-switch DC-DC boost converter are analyzed. The DC motor is operated at no-load condition. The converter is operated in continuous inductor current mode. The duty ratio (D) of the MOSFET switch 'S' is adjusted gradually to vary the armature voltage of the motor quadratically, which in turn changes the speed of the DC motor. As the applied voltage control scheme is used, the speed variations are approximately proportional to the armature voltage variations. The performance of the proposed converter-fed DC motor is validated for the duty ratio (D=0.71), using MATLAB/SIMULINK tool. The various performance characteristics of the motor are obtained under no-load condition. The no-load speed control characteristics of the motor are too obtained for varying armature voltages with respect to changes in duty ratio (D). The significant feature of the no-load speed control by the proposed converter-fed DC motor is that the proposed high-gain converter topology employs single power switch, which in turn improves the converter efficiency by reducing the switching and conduction losses.

#### ACKNOWLEDGEMENT

The authors acknowledge the help provided by the Department of Electrical and Electronics Engineering, Government College of Engineering, Salem, in carrying out the research work on the proposed converter-fed DC motor.

#### REFERENCES

1. M. A. Chewale, R. A. Wanjari, V. B. Savakhande, and P. R. Sonawane. **A review on isolated and non-isolated DC-DC converter for PV application**, *International Conference on Control, Power, Communication and Computing Technologies (ICCPCT)*, pp. 399-404, March 2018.
2. F. Mumtaz, N. Z. Yahaya, S. T. Meraj, B. Singh, Ramani Kannan, and O. Ibrahim. **Review on non-isolated DC-DC converters and their control techniques for renewable energy applications**. *Ain Shams Engineering Journal*, vol. 12, no. 4, pp. 3747-3763, December 2021.
3. A. Chub, D. Vinnikov, F. Blaabjerg, and F. Z. Peng. **A review of galvanically isolated impedance-source DC-DC converters**. *IEEE Transactions on Power Electronics*, vol. 31, no. 4, pp. 2808-2828, April 2016.
4. F. L. Tofoli, D. d. C. Pereira, W. J. de Paula, and D. D. S. Oliveira Junior. **Survey on non-isolated high-voltage step-up dc-dc topologies based on the boost converter**. *IET Power Electronics*, vol. 8, no. 10, pp. 2044-2057, July 2015.
5. F. M. Shahir and E. Babaei. **Extended topology for a boost DC-DC converter**. *IEEE Transactions on Power Electronics*, vol. 34, no. 3, pp. 2375-2384, March 2019.
6. V. Girija and D. Murali. **Simulation and steady state analysis of a non-isolated diode rectifier-fed DC-DC boost converter with high static voltage gain**. *International Journal for Modern Trends in Science and Technology*, vol. 7, no. 3, pp. 20-25, March 2021.
7. M. Forouzesh, Y. Shen, K. Yari, Y. P. Siwakoti, Y.P. and F. Blaabjerg. **High-efficiency high step-up dc-dc converter with dual coupled inductors for grid-connected photovoltaic systems**. *IEEE Transactions on Power Electronics*, vol. 33, no. 7, pp. 5967-5982, July 2018.
8. C. Si, Z. Luowei, L. Quanming, G. Wei, W. Yuqi, S. Pengju, and D. Xiong. **Research on topology of the high step-up boost converter with coupled inductor**. *IEEE Transactions on Power Electronics*, vol. 34, no. 11, pp. 10733-10745, November 2019.
9. W. Hanging, G. Arnaud, and H. Daniel. **A review of DC/DC converter-based electrochemical impedance spectroscopy for fuel cell electric vehicles**. *Renewable Energy*, vol. 141, pp. 124-138, October 2019.
10. V. F. Pires, A. Cordeiro, D. Foito, and J. F. Silva. **High step-up DC-DC converter for fuel cell vehicles based on merged Quadratic boost-Cuk**. *IEEE Transactions on Vehicular Technology*, vol. 68, no. 8, pp. 7521-7530, August 2019.
11. Y. Zhang, H. Liu, J. Li, M. Sumner, and C. Xia. **DC-DC boost converter with a wide input range and high voltage gain for fuel cell vehicles**. *IEEE Transactions on Power Electronics*, vol. 34, no. 5, pp. 4100-4111, May 2019.

12. A. A. M. Ferdowsi and P. Shamsi. **High-voltage-gain DC-DC step-up converter with Bifold Dickson voltage multiplier cells.** *IEEE Transactions on Power Electronics*, vol. 34, no. 10, pp. 9732-9742, October 2019.
13. U. Rafiq, A. F. Murtaza, H. A. Sher, and D. Gandini. **Design and analysis of a novel high-gain DC-DC boost converter with low component count.** *Electronics*, vol. 10, pp. 1-15, July 2021.
14. P. S. Bimbhra, *Electrical Machinery*, 7<sup>th</sup> ed., Khanna Publishers, New Delhi, 1993, Ch. 4, pp. 455-488.